*Acta Oceanologica Sinica* 2008, Vol. 27, Supp., p. 74 ~ 92
http://www.oceanpress.com.cn
E-mail: hyxbe@263.net

# A generic approach to the dynamical interpretation of ocean-atmosphere processes

X. San Liang[1*]

1. Courant Institute of Mathematical Sciences, New York, New York 10012, USA

Received 14 January 2006; accepted 21 June 2006

**Abstract**

This paper summarizes the recent development of a portable self-contained system to unravel the intricate multiscale dynamical processes from real oceanic flows, which are in nature highly nonlinear and intermittent in space and time. Of particular focus are the interactions among largescale, mesoscale, and submesoscale processes. We first introduce the concept of scale window, and an orthogonal subspace decomposition technigue called multiscale window transform (MWT). Established on MWT is a rigorous formalism of multiscale transport, perfect transfer, and multiscale conversion, which makes a new methodology, multiscale energy and vorticity analysis (MS-EVA). A direct application of the MS-EVA is the development of a novel localized instability analysis, generalizing the classical notion of hydrodynamic instability to finite amplitude processes on irregularly variable domains. The theory is consistent with the analytical solutions of Eady's model and Kuo's model, the benchmark models of baroclinic instability and barotropic instability; it is further validated with a vortex shedding control problem. We have put it to application with a variety of complicated real ocean problems, which would be otherwise very difficult, if not impossible, to tackle. Briefly shown in this paper include the dynamical studies of a highly variable open ocean front, and a complex coastal ocean circulation. In the former, it is found that underlying the frontal meandering is a convective instability followed by an absolute instability, and correspondingly a rapid spatially amplifying mode locked into a temporally growing mode; in the latter, we see a real ocean example of how upwelling can be driven by winds through nonlinear instability, and how winds may excite the ocean via an avenue which is distinctly different from the classical paradigms. This system is mathematically rigorous, physically robust, and practically straightforward.

**Key words**: Multiscale energy and vorticity analysis, multiscale window transform, multiscale transport, perfect transfer, finite-amplitude hydrodynamic instability analysis, mean-eddy-turbulence interaction

## 1 Introduction

During the past few years, a self-contained system, multiscale energy and vorticity analysis (MS-EVA), has been developed for the interpretation of the complex multiscale dynamical processes in the ocean (Liang, 2002; Liang and Robinson, 2005; Liang and Robinson, 2007; Liang, 2008). Based on a new analysis aparatus, multiscale window transform (Liang and Anderson, 2007), it bears generality and objectivity; in other words, it applies to problems

* Corresponding author, E-mail: san@deas.harvard.edu

on a generic basis, and provides quantitative results rather than qualitative information. This system has been utilized for real ocean operations and dynamical studies (Liang and Robinson, 2004; Liang and Robinson, 2008)[1]. It is now an integrated component of the Harvard Ocean Prediction System (HOPS) (e. g. Lozano, et al. 1996).

The establishment of the system is mainly motivated by the imperative need of dynamical diagnostics as oceanographic data keep building up. We have entered an era of data wealth. A major task of the next generation of oceanography would be how to interpret these data. So far, on one hand, we have geophysical fluid dynamics (GFD) theories, many of them developed on classical analysis tools which are global in characteristic; on the other hand is the real ocean, processes in nature locally structured and windowed on scales (i. e., occurring on a range of scales). A gap, therefore, exists between these theories and real problems. We have been attempting to generalize the existing GFD theories to fill the gap; the development of the MS-EVA makes such an attempt. This review gives it a brief expository introduction. Detailed mathematical derivations are avoided, and those who feel interested are referred to the references cited in the text.

Multiscale phenomena are ubiquitous in the ocean. This arises from the field, space and time, over which ocean state variables are defined. The effect of the field may be seen in the magic formation of multiscale patterns when a chemical reaction (zero - dimensional) is recast on a field (2D or 3D space), i. e., to allow for spatial distribution (e. g., the Belonsov-Zhabotinsky system (Vanag et al., 2001)); even though the reaction is very simple, the patterns may appear complex. The MS-EVA is to investigate how the multiscale complexity arises, through different realizations in the ocean. Related problems include eddy shedding, jet meandering, emergence of coherent structures, hydrodynamic instabilities, turbulent transition, dispersion of chemical constituents, to name but a few.

Underlying these problems there is something in common but more fundamental, which makes what we are interested from the viewpoint of multiscale dynamics as a branch of science. To illustrate, suppose a state variable $f$ lies in a Hilbert space $\Omega \subset L_2$ over some definition domain.[2] Under some dynamics, which we abstractly write as a map $\Phi$, $\Omega$ is sent to another space $\omega$, as schematized in Fig. 1. Suppose we have a decomposition for $\Omega = \Omega_0 \oplus \Omega_1 \oplus \Omega_2$, which is fulfilled according to some rule with respect to scale, such that they contain largescale, mesoscale, and submesoscale processes, respectively. The resulting three suspaces $\Omega_0$, $\Omega_1$, and $\Omega_2$ are orthogonal or mutually exclusive. They are brought to $\omega_0$, $\omega_1$ *and* $\omega_2$, respectively, as $\Phi$ sends $\Omega$ to $\omega$. As we will detail later, when $\Phi$ is nonlinear, $\omega_0$, $\omega_1$ and $\omega_2$ are no longer mutually exclusive. The objective of multiscale ocean dynamics study is, therefore, to investigate how a property is transported within their individual subspaces, and redistributed through the overlapping or interaction upon applying the dynamics. The transport and redistribution are the very multiscale transport and interscale transfer, which we will elaborate soon.

We will need to decide what property to choose for the multiscale transport and redistribution. As the essence of this research lies in the interactions among $\Omega_i$ ($i = 0, 1, \cdots$), the property should be characteristic of these subspaces. In the $L_2$ framework, a function is a "vector"; one cannot directly compare a vector with another vector. There should be some metric for the comparison to realize. This

1) An application package is available upon request.

2) An $L_2(\Pi)$ is, loosely speaking, a space made of functions quadratically integrable over domain $\Pi$. This concept is not essential for the treatment of the material. We use it here for some justification later. The reader may simply skip it.

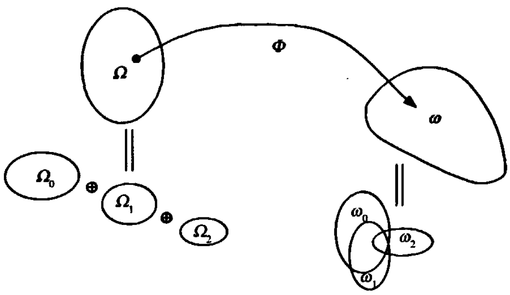


Fig. 1. A schematic of the multiscale ocean dynamics.

metric is norm (more generically inner product), which corresponds to energy in physics. So the natural choice of the property is energy. In the context of geophysical fluid dynamics we specifically need to deal with kinetic energy, available potential energy, and enstrophy ("vorticity energy"). That is the reason why the system earns its name, multiscale energy and vorticity analysis,[3)] or MS-EVA for short.

In the following we address the issues in achieving the multiscale decomposition, and thereby the establishment of a variety of formalisms. We first introduce the mathematical framework, then the derivation of MS-EVA, based on which a novel localized hydrodynamic instability analysis is developed. The whole theory is validated with well known idealized models, and put to application with real ocean problems. In the last section, some unresolved issues are discussed and application prospects supplied.

## 2 Multiscale window transform

Here we introduce a new mathematical apparatus, multiscale window transform, to fulfill the decomposition illustrated in Fig. 1. All the theoretical details about the development will be dropped. Those who do not want to get into the mathematical aspect may skip this part: It is enough just to be familiar with some of the notations.

Different scale analyses may yield different state variable decompositions. In Liang and Anderson (2007) and Liang and Robinson (2005), we argued that the classical approaches, such as the Fourier analysis and the average-departure separation, are not applicable in this case because of the inconsistency between decomposition and energy localization. The resulting multiscale energy does not bear information of locality in those frameworks. Modern techologies, such as wavelet analysis (Holschneider, 1995) and Hilbert-Huang transform (Huang et al., 1999), offer a solution to this problem. The Hilbert-Huang transform is for different uses (see Liang and Anderson, 2007 for comparison); wavelet analysis almost makes a candidate save for a reason we hereafter elucidate.

Recall that we are dealing with energy, the candidate decomposition should be orthogonal, otherwise the resulting energy will not be conserved. Besides, an ocean process tends to occur on a scale window or a range of scales, instead of a single scale. A good example is turbulence. It has an inertial range which is scale free, i.e., without a characteristic scale (Chorin, 1994). We therefore need to study problems on different windows rather than individual scales. For orthonormal wavelet analysis, the transform coefficients are defined discretely on physical space locations for different scales, as schematized in Fig. 2, at the mesh points (Holschneider, 1995). There is no way to take summation of energy (square of the transform coefficients multiplied by some factor) at a specific location over the scale indices to make a scale window. Thus wavelet analysis is not appropriate for our purpose.

3) We do not call it "multiscale energy and enstrophy analysis" because there is a historic account of energy and vorticity analysis (EVA) (Spall, 1989; Pinardi and Robinson, 1986).

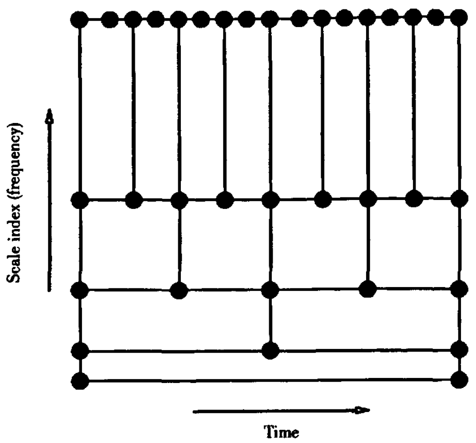


**Fig. 2.** Schematic of the multiresolution of time-frequency plane decomposition using an orthonormal wavelet basis. The wavelet transform coefficients (hence energies) are defined at the nodes of the board, which are discretely located at different time points for different frequencies.

We therefore need our own analysis tool. We need a tool such that energy is represented at different physical locations for different scale windows. Take a 1D function $f(t) \subset L_2[0,1]$ as an example. (Higher dimensional problems are much more complicated and the reader is referred to Liang, 2002). Without loss of generality, the definition domain is chosen as $[0,1]$. If not, one may always change it through a simple variable transformation. Liang and Anderson (2007) justified that, any signal $f(t)$ taken from observations or experiments (either numerical or physical) lie in a subspace $f(t)$ which is spanned by a translation invariant basis[4)]

$$\{\phi_n^{j_2}\} = \{\sum_{l=-\infty}^{\infty} \phi[2^{j_2}(t+l) - n]\}, \quad n = 0,1,\cdots,2^{j_2}-1, \tag{1}$$

for sufficiently large but finite integer $j_2$. Here $\phi(t)$ is a scaling function orthonormalized from cubic splines (Liang, 2002), as shown in Fig. 3. From $V_{j_2}$ we may rigorously introduced the concept of large-scale, mesoscale, and submesoscale windows, characterized by three integers or scale indices $j_0$, $j_1$ and $j_2$. These windows are subspaces of $V_{j_2}$, containing processes of scales ranging from $2^{-j_0}$-1, $2^{-j_1}$-$2^{-j_0}$, and $2^{-j_2}$-$2^{-j_1}$, respectively. A rigorous treatment can be seen in Liang and Anderson (2007). For convenience, we may alternatively refer these windows as windows 0, 1, and 2.

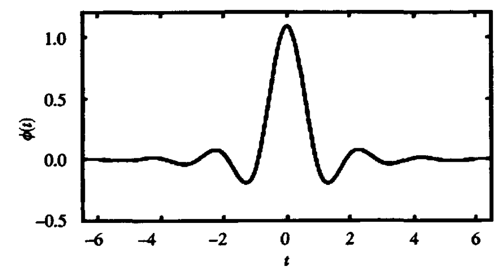


**Fig. 3.** Scaling function constructed from the cubic spline.

Given $f \in V_{j_2}$, there is a scaling transform

$$\hat{f}_n^j = \int_0^1 f(t)\phi_n^j(t)\,dt, \tag{2}$$

for $0 \leqslant j \leqslant j_2$, $n = 0,1,\cdots,2^j-1$. Given $0 \leqslant j_0 \leqslant j_1 \leqslant j_2$, the scaling transform can be used to construct the following three functions:

$$\hat{f}^{\sim 0}(t) = \sum_{n=0}^{2^{j_0}-1} \hat{f}_n^{j_0}\phi_n^{j_0}(t), \tag{3}$$

$$f^{\sim 1}(t) = \sum_{n=0}^{2^{j_1}-1} \hat{f}_n^{j_1}\phi_n^{j_1}(t) - f^{\sim 0}(t), \tag{4}$$

$$f^{\sim 2}(t) = f(t) - \sum_{n=0}^{2^{j_1}-1} \hat{f}_n^{j_1}\phi_n^{j_1}(t). \tag{5}$$

They are called, respectively, reconstructions of $f(t)$ on windows 0, 1 and 2, and accordingly represent the largescale, mesoscale, and submesoscale parts of $f(t)$. The corresponding multiscale window transforms (MWT) are

$$\hat{f}_n^{\sim \varpi} = \int_0^1 f^{\sim \varpi}(t)\phi_n^{j_2}(t)\,dt, \quad \text{for } \varpi = 0,1,2; \quad n = 0,1,\cdots,2^{j_2}-1, \tag{6}$$

4) The generic form is more complex. Here we consider only the simple case with a periodic extension scheme for $\phi$.

which make three transform – reconstruction pairs together with Eqs(3) – (5).

The MWT has some nice properties. Shown below are two which we will have a chance to use later in this paper:

**Theorem 1** If $j_0 = 0$, then

$$f^{\sim 0}(t) = \int_0^1 f(t)\,dt = \bar{f}; \quad (7)$$

$$f^{\sim 1}(t) + f^{\sim 2}(t) = f - \bar{f} = f', \quad (8)$$

where the overbar is for the average over the definition domain.

**Theorem 2**

$$\overline{f^{\sim\varpi}(t) \cdot g^{\sim\varpi}(t)} = \sum_{n=1}^{N-1} \hat{f}_n^{\sim\varpi} \hat{g}_n^{\sim\varpi} + \frac{1}{2}(\hat{f}_0^{\sim\varpi} \hat{g}_0^{\sim\varpi} + \hat{f}_N^{\sim\varpi} \hat{g}_N^{\sim\varpi}) = M_n(\hat{f}_n^{\sim\varpi} \hat{g}_n^{\sim\varpi}), \quad N = 2^{j_2}, \quad (9)$$

for $\varpi = 0, 1, 2$.

In (9), $M_n$ is called a marginalization over the locations $n$, and Theorem 2 is accordingly called *property of marginalization*. This property allows energy to be simply represented as the square of MWT transform coefficients, up to some constant factor depending on the context.

To end this section, we present the MWT analysis of a time series extracted from an island wake simulation within the near wake (Liang and Wang. 2004). We just briefly take a look at the reconstructions for different windows, without touching any details. Clearly, the largescale feature ($u^{\sim 0}$) has a time dependence, i. e., it is nonstationary. More interesting is the mesoscale process ($u^{\sim 1}$). It is under a rapid growth, implying that some instability is occurring. The remaining window contains all other processes with short scales, which appear in a way with stochasticity. The energies of these processes also vary in time, following roughly similar patterns corresponding to $u^{\sim 0}$, $u^{\sim 1}$, and $u^{\sim 2}$, which we do not show here. The analysis is fulfilled very effectively, using a fast algorithm developed in Liang (2002) and Liang and Anderson (2007).

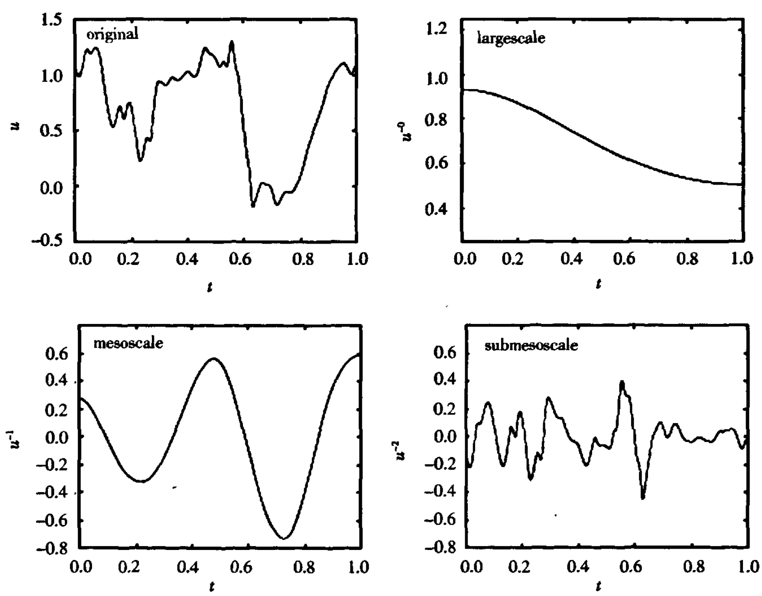


Fig. 4. Largescale, mesoscale, and submesoscale reconstructions of a time series of $u$ (top-left). Both the variables, $u$ and $t$ are nondimensionalized. [Adopted from Liang and Wang (2004)].

## 3 Multiscale energy and vorticity analysis

The objective of multiscale ocean dynamics analysis, in general language, is to investigate how the individual scale windows as shown in Fig. 1 evolve under the dynamics, and how they interact with each other in the course of evolution. As we argued before, what characterize these windows are their respective norms in mathematics, or energies in physics. Energy is also the metric we can utilize to make comparisons between the subspaces (windows) before and after the dynamics applies. The objective is, therefore, translated into the investigation of how energy grows on a specific window, via transports from within, transfers from without, and, if any, conversions between different types of energy.

The law of energy growth on multiple scale windows is derived from the Navier-Stokes equations for the Bousinesq ocean with a hydrostatic assumption:

$$\frac{\partial \underline{v}_h}{\partial t} = -\nabla \cdot (\underline{v}\underline{v}_h) - f\underline{k} \wedge \underline{v}_h - \frac{\nabla P}{\rho_0} + \underline{F}_m, \quad (10)$$

$$0 = \nabla \cdot \underline{v}, \quad (11)$$

$$0 = -\frac{\partial P}{\partial z} - \rho g, \quad (12)$$

$$\frac{\partial \rho}{\partial t} = -\nabla \cdot (\underline{v}\rho) + \frac{N^2 \rho_0}{g} w + F_\rho, \quad (13)$$

where $\underline{v} = (u, v, w)$, $\nabla = \underline{i}\frac{\partial}{\partial x} + \underline{j}\frac{\partial}{\partial y} + \underline{k}\frac{\partial}{\partial z}$, $N = \left(-\frac{g}{\rho_0}\frac{\partial \bar{\rho}(z)}{\partial z}\right)^{1/2}$ is the buoyancy frequency, $\rho$ the density anomaly (with $\rho_0$ = const and $\bar{\rho} = \bar{\rho}(z)$ excluded), subscript h the horizontal component of a 3D vector. The $F$ terms stand for the dissipation/diffusion processes which we will not explore in this review. Other symbols are conventional.

To start, we first need to perform MWT decomposition. This may be achieved either in time or in space. They are observed equivalent. We choose to perform in time in order to avoid the possible scale ambiguity when nonlinearity takes effect to organize the processes into coherent structures, which may have different scales in different spatial dimensions. (A spatial scale makes sense only when the flow is isotropic). Besides, it is a convention in GFD research that scales are defined in time: the conceptualization has been useful in meteorology.

Now suppose the time sequences have a length of $2^{j_2}$ time points. Then the problem can be studied in $V_{j_2}$, the space spanned by $\{\phi(2^{j_2}t - n\}_{n \in Z}$. Consider three scale windows, denoted subsequently 0, 1 and 2 which correspond to the largescale, mesoscale, and submesoscale processes in the ocean. (More windows can be decomposed but three are usually enough for ocean processes.)

Define

$$K_n^\varpi = 2^{j_2}\left(\frac{1}{2}\hat{\underline{v}}_n^{\sim\varpi} \cdot \frac{1}{2}\hat{\underline{v}}_n^{\sim\varpi}\right), \quad (14)$$

$$A_n^\varpi = 2^{j_2}\left(\frac{1}{2}c\hat{\rho}_n^{\sim\varpi} \cdot \hat{\rho}_n^{\sim\varpi}\right) \quad (15)$$

as the kinetic and available potential energies for window $\varpi$ ($\varpi = 0,1,2$) and time step $n$, where $c = g^2/[\rho_0^2 N^2]$. Here $j_2$ is the largest scale index admissible for the time sequences. The factor $2^{j_2}$ is needed to make contact with the energy in the physical sense (Liang and Robinson, 2005), but for notation brevity, we will omit it from the expressions henceforth. It is easy to prove, using the marginalization property of the MWT, that the energy thus defined is conserved.

The evolutions of $K_n^\varpi$, $A_n^\varpi$, for $\varpi = 0,1,2$, and all the time steps $n$ can be obtained by taking MWT on both sides of Eqs(10) and (13), followed by a multiplication of $\hat{\underline{v}}_n^{\sim\varpi}$ and $c\hat{\rho}_n^{\sim\varpi}$, respectively. The derivation is beyond the scope of this review. We just show the results here. With the aid of Eqs(11) and (12), and the related properties of MWT, we arrive at the following equations:

$$\dot{K}_n^{\varpi} = \Delta Q_{K_n^{\varpi}} + \Delta Q_{P_n^{\varpi}} + T_{K_n^{\varpi}} - b_n^{\varpi} + \text{diss.}, \quad (16)$$

$$\dot{A}_n^{\varpi} = \Delta Q_{A_n^{\varpi}} + T_{A_n^{\varpi}} + b_n^{\varpi} + \text{diff.}, \quad (17)$$

where diss. and diff. signify the dissipation and diffusion processes we do not consider here. Among other terms,

$$b_n^{\varpi} = \frac{g}{\rho_0} \hat{w}_n^{\sim\varpi} \hat{\rho}_n^{\sim\varpi} \quad (18)$$

is the rate of buoyancy conversion,

$$\Delta Q_{P_n^{\varpi}} = -\nabla \cdot \left( \hat{\underline{v}}_n^{\sim\varpi} \frac{\hat{P}_n^{\sim\varpi}}{\rho_0} \right) \quad (19)$$

the pressure working rate, and

$$\Delta Q_{P_n^{\varpi}} = -\nabla \cdot [\lambda \hat{\underline{v}}_n^{\sim\varpi} \cdot (\widehat{\underline{v}\underline{v}_h})_n^{\sim\varpi}] \quad (20)$$

$$\Delta Q_{A_n^{\varpi}} = -\nabla \cdot [\lambda \, \widehat{c\rho}_n^{\sim\varpi} \cdot (\widehat{\underline{v}\rho})_n^{\sim\varpi}] \quad (21)$$

the transport of $K$ and $A$ on window $\varpi$ at step $n$. The remaining terms are transfers across different windows:

$$T_{K_n^{\varpi}} = -\lambda [(\hat{u}_n^{\sim\varpi})^2 \nabla \cdot \underline{v}_u + (\hat{v}_n^{\sim\varpi})^2 \nabla \cdot \underline{v}_v,] \quad (22)$$

$$T_{A_n^{\varpi}} = -2\lambda A_n^{\varpi} \nabla \cdot \underline{v}_\rho, \quad (23)$$

where

$$\underline{v}_s = \frac{(\widehat{S\underline{v}})_n^{\sim\varpi}}{\hat{S}_n^{\sim\varpi}} \quad (24)$$

for $S = u$, $v$, or $\rho$. The variable $\underline{v}_s$ has the dimension of velocity; we will hereafter refer to it as $S$-velocity. It has been proved that (Liang and Robinson, 2005)

$$M_n \sum_n T_n^{\varpi} = 0 \quad (25)$$

for either $T_n^{\varpi} = T_{K_n^{\varpi}}$ or $T_n^{\varpi} = T_{A_n^{\varpi}}$, if and only if the coefficient $\lambda$ equals 1/2. The transfer processes such that Eq. (25) holds are called *perfect transfers*.

Perfect transfer is an important concept in multiscale ocean dynamics. It is an energy redistribution process among the scale windows, in that no energy is generated or destroyed as a whole. It is thus a faithful measure of the interaction between scale windows. The conceptualization of Eq. (25) eliminates the ambiguity in quantifying transfer processes by casting the concept on a rigorous footing of mathematics and robust ground of physics.

Transfers are generally interwoven with transports due to the nonlinear nature of the N-S equations. They are separated out from the coupling with the aid of Eq. (25). This technique, which is made precise in the framework of MWT, has been termed "transport – transfer separation" by Liang and Robinson (2005). The $Q$ terms listed above, $\Delta Q_{P_n^{\varpi}}$, $\Delta Q_{K_n^{\varpi}}$, and $\Delta Q_{A_n^{\varpi}}$ are representations of the multiscale transports. Note that $\Delta Q_{K_n^{\varpi}}$ and $\Delta Q_{A_n^{\varpi}}$ involve not only fields from the window $\varpi$, but also from other windows. The expanded version is in general quite complicated and we refer the reader to Liang and Robinson (2005) for details.

The other energetic process is the conversion between kinetic energy and available potential energy through buoyancy work. It is represented by $b_n^{\varpi}$ in Eqs (16) and (17). Compared with its transport and transfer counterparts, buoyancy conversion is relatively simple. It occurs on individual windows only, without invoking energy exchange in between.

To summarize, Fig. 5 presents a chart of the energy flow for a two – window decomposition. These two windows, windows 0 and 1, may be understood as, respectively, the largescale window or "mean" window, and the mesoscale or "eddy" window. From the flow chart the perfect transfers (marked as $T_A$ add $T_K$) act as two protocols in phase space between the mean structure and the eddy structure, while the transports are processes occurring in physical space within each individual window. The APE and KE on each window are simply connected through the corresponding buoyancy conversion. Energy flows for decompositions with three or more windows are much more complex and are referred to Liang and Robinson (2005).

## 4 Hydrodynamic instability analysis

The concept of hydrodynamic instability, baro-

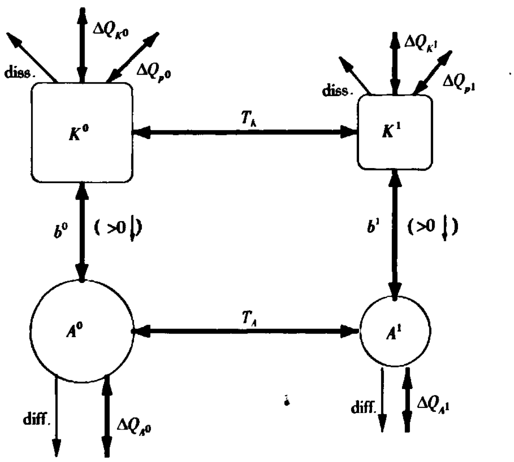


Fig. 5. A schematic of the energetics for a two-window decomposition. The symbols are basically the same as those in Eqs(16) and (17), except that the subscript $n$ (time step) is omitted for simplicity. The windows 0 and 1 may be understood as, respectively, the largescale window and mesoscale window (or "eddy" window).

tropic instability and baroclinic instability in particular, is very important in geophysical fluid dynamics. Like any infinite dimensional dynamical processes (Temam, 1997), hydrodynamic instabilities tend to be localized in space and time. This is especially apparent in the ocean and atmosphere, where processes are generally highly nonlinear and are often organized into coherent structures over finite, irregular, and mobile domains. Traditionally, however, stability is a notion over a system (e.g. Lin, 1966; Drazin and Reid, 1982). There is no way to distinguish these localized coherent structures. To remedy the difficulty, alternative conceptualizations have been sought based on different approximations within the corresponding contexts. An effort is the parcel stability analysis, which has been successfully utilized to investigate symmetric instabilities in the atmosphere (cf. Holton, 1992). The WKB formalism on convective and absolute instabilities is another effort (e.g., Huerre and Monkewitz, 1990; Pierrehumbent and Swanson, 1995). Examples in other disciplines may be found in the research of localized standing Rankine – Hugoniot shocks (Chakrabarti, 1989) and the studies of plasma instability (Chu et al., 1996). These analyses, albeit localized, are either Lagrangian or rest on the assumption of small perturbation. We still lack an approach to these processes on a generic basis, particularly instabilities of finite amplitude, within the Eulerian framework. In the following, we show how the MS-EVA developed before may come to help to give this old problem a unified solution.

### 4.1 Formalism

A loose but intuitive approach toward the formalism of a localized instability analysis is through making analogy with the classical definition in terms of perturbative energy growth (Liang and Robinson, 2007). In this way the two important GFD concepts, barotropic instability and baroclinic instability, can be easily generalized onto a generic basis, as we will demonstrate in the following. A rigorous formalism in the sense of Lyapunov is also possible; referred to Liang et al. (2008) for details.

Classically, instabilities correspond to the growth of disturbances, and thereby, GFD instabilities can be defined with the linearized growth equation of perturbation energy. In the context of a zonal jet stream with a rigid lid, the linear eddy energy $E_{eddy}$ grows as (Cushman-Rosin, 1994; Holton, 1992; Pedlosky, 1979):

$$\frac{\partial \langle E_{eddy} \rangle^{\Omega}}{\partial t} = - \left\langle \frac{fg}{\rho_0 N^2} \overline{v'\rho'} \frac{\partial \bar{u}}{\partial z} \right\rangle^{\Omega} + \left\langle - \overline{u'v'} \frac{\partial \bar{u}}{\partial y} - \overline{u'w'} \frac{\partial \bar{u}}{\partial z} \right\rangle^{\Omega}$$

$$\equiv \langle BC^* \rangle^{\Omega} + \langle BT^* \rangle^{\Omega}, \qquad (26)$$

where $\langle \cdot \rangle^{\Omega}$ is an average over the basin $\Omega$ confined between two latitudes; an overbar stands for an ensemble mean which practically is replaced by a time average, a prime is a departure from the mean, and other notations are conventional. The two parts on the right hand side are denoted as $\langle BC^* \rangle^\Omega$ and $\langle BT^* \rangle^\Omega$ for later use.

Two types of instabilities may be distinguished by the relative importance of $\langle BC^* \rangle^\Omega$ versus $\langle BT^* \rangle^\Omega$ to the growth of $\langle E_{eddy} \rangle^\Omega$. If the increase of $\langle E_{eddy} \rangle^\Omega$ is due to $\langle BC^* \rangle^\Omega$, then the system is undergoing a baroclinic instability, otherwise a barotropic instability. Note here $\langle BC^* \rangle^\Omega$ and $\langle BT^* \rangle^\Omega$ are two quantities averaged both in time and in space. They are just two numbers for the whole domain over the whole duration of concern. It is impossible to distinguish local processes (such as hurricanes or ocean eddies) from one location to another. In other words, adopting Eq. (26) to define instability tacitly invokes two assumptions: homogeneity and stationarity. But, ironically, instabilities are in nature neither homogeneous nor stationary!

The difficulty with the classical definition lies in the avearges in the two instability metrics, $\langle BC^* \rangle^\Omega$ and $\langle BT^* \rangle^\Omega$. One may naturally asks whether they can be relieved. This, of course, cannot be done directly, or the resulting energetics will be physical meaningless (energetics in the classical sense must bear these averages). But it offers an important clue. Our strategy here is to localize $\langle BC^* \rangle^\Omega$ and $\langle BT^* \rangle^\Omega$ such that they become two 4D field variables. This way one need not be concerned about whether there are any local events taking place in the domain, nor need he worry about which period to choose in order to capture the events in time. Besides, irregular and mobile definition domain and nonstationary background will also be accommodated in a unified treatment.

To localize, recall that if the low-window bound $j_0 = 0$ (and a periodic extension is used), and only two windows are taken into account, the reconstructions are then precisely the time mean and the departure from the mean. With this decomposition, it has been proved that $\langle BC^* \rangle^\Omega$ and $\langle BT^* \rangle^\Omega$ can be accordingly rewritten in terms of the transfers introduced in the preceding section (Liang and Robinson, 2007), and particularly,

$$\langle BC^* \rangle^\Omega = \langle M_n T_{A_n^1} \rangle^\Omega, \qquad (27)$$

$$\langle BT^* \rangle^\Omega = \langle M_n T_{K_n^1} \rangle^\Omega, \qquad (28)$$

where $\varpi = 1$ stands for the "eddy window". Notice the MS-EVA quantities $T_{A_n^1}$ and $T_{K_n^1}$ are concepts independent of the marginalization $M_n$ and the domain average $\langle \cdot \rangle^\Omega$, and so the two operators can be relieved. Our task for the next step is to relax $M_n$ and $\langle \cdot \rangle^\Omega$, to obtain two new instability metrics as functions of space and time. We fulfill these one by one:

(1) *Localization in space: transport-transfer separation.* Relaxation of $\langle \cdot \rangle^\Omega$ corresponds to localization in space. The resulting metric is unique up to a term in the divergence form. Recall we have performed a transport – transfer separation through introducing the physically robust concept of perfect transfer. The perfect transfer is thus what we expect. Relaxation of $\langle \cdot \rangle^\Omega$ eliminates the boundary constraints, as a result the analysis can be applied to problems on domains of arbitrary geometry.

(2) *Localization in time: interaction analysis.* Relaxation of the marginalization gives a result unique up to a term $G_n$ such that $M_n G_n = 0$, i. e., the transfers within the same window. To eliminate this underterminism, one needs to remove from the perfect transfers the contributions from within the same window, so as for the transfers from the background (window 0) to the eddy window (window 1) to come up front. Liang and Robinson (2005) used a technique called interaction analysis to achieve this elimination. Here we just write it symbolically as a superscript $0 \to 1$, which signifies an operator selecting out the transfers from window 0 to window 1. Relaxation of $M_n$ prohibits the analysis from messing up with temporally irrelevant processes.

We then obtain two new metrics, denoted as $BC$ and $BT$, for instability identification:

$$BT = T_{K_n^1}^{0 \to 1}. \qquad (29)$$

$$BC = T_{A_n^1}^{0\to1}. \tag{30}$$

They correspond to the $\langle BT^* \rangle^{\Omega}$ and $\langle BC^* \rangle^{\Omega}$ in Eq. (26), respectively. In analogy to the classical instability definition, we have an easy-to-use criterion for instability identification (Liang and Robinson, 2004; Liang and Robinson, 2007):

(1) A flow system is locally stable if $BT + BC < 0$, neutrally stable if $BT + BC = 0$, and unstable otherwise;

(2) For an unstable system, if $BT > 0$ and $BC \leqslant 0$, the instability the system undergoes is barotropic;

(3) For an unstable system, if $BC$ is positive but $BT$ is not, then the instability is baroclinic;

(4) If both $BT$ and $BC$ are positive, the system must be undergoing a mixed instability.

In the formalism, both $BT$ and $BC$ are variables on the 4D time-space field. Spatially localized and temporally episodic events are thus naturally embedded. Besides, the relaxed $BC$ and $BT$ do not have the constraint $j_0 = 0$, i. e., nonstationary backgrounds are automatically incorporated. In other words, the criterion is applicable to generic ocean problems. For convenience, we may loosely refer to BC and BT as "baroclinic transfer" and "barotropic transfer".

### 4.2 Horizontal treatment

As a localized transform, the MWT in time may give rise to phase error in the horizontal due to Galilean transformation. This is a problem similar to that of wavelet analysis as pointed out by Lima and Toh (1995) for the wavelet transform. In this case, as shown in Liang and Robinson (2005), it affects only the highest scale levels, and so the error can be removed from the calculated $BT$ and $BT$ through a horizontal low-pass filtering. In the rigorous Lyapunov formalism, this horizontal treatment corresponds to a localized spatial average, which is needed in finding the norm to measure localized instability.

### 4.3 Connection to the classical $BT$

It should be noted that, although $BT$ and $BC$ are derived by making analogy to Eq. (26) with $BT^*$ and $BC^*$. $BT$ (resp. $BC$) is by no means a generalization of $BT^*$ (resp. $BC^*$) on a localized basis. They are in fact fundamentally different metrics. Taking $BT$ as an example. One may see the difference by setting $j_0 = 0$, and making comparison between $BT$ and $BT^*$. (Only when $j_0 = 0$ may the two be compared, as in this case a two-window analysis is reduced to the mean-departure decomposition.) In the case of a basic flow $(u(y), 0, 0)$, $BT$ becomes (Liang and Robinson, 2007)

$$BT = \frac{1}{2}\left[\bar{u}\frac{\partial \overline{u'^2}}{\partial x} + \bar{u}\frac{\partial \overline{u'v'}}{\partial y} - \overline{u'v'}\frac{\partial \bar{u}}{\partial y}\right], \tag{31}$$

while

$$BT^* = -\overline{u'v'}\frac{\partial \bar{u}}{\partial y}. \tag{32}$$

The difference may yield quite different instability scenarios for the same problem. We refer the reader to Liang and Robinson. (2007) for details.

### 4.4 An alternative formalism

Notice in Fig. 5, the perfect transfers are protocols between two windows. Their status is two-fold, depending on where the observer stands to interpret them. Look at $T_{K_n^{\cdot}}$. If we are interested in the energy transfer from the largescale window to the eddy window, as in the case of hydrodynamic instability analysis, we may either have $T_{K_n^1}^{0\to1}$ or $T_{K_n^0}^{0\to1}$ as the metrics. The former is the $BT$ introduced above. It represents a transfer process based on window 1 (the eddy window). What is the latter? It is essentially the same process, but rooted in window 0. So we may equally define two quantities (Liang and Robinson, 2005)

$$BT = T_{K_n^0}^{0\to1} = -T_{K_n^0}^{1\to0} \tag{33}$$

$$BC = T_{A_n^0}^{0\to1} = -T_{A_n^0}^{1\to0} \tag{34}$$

as respective metrics for baroclinic instability and barotropic instability. In general, Eq. (33) [resp. Eq. (34)] and Eq. (29) [resp. Eq. (30)] are not identical, but when marginalized they are the same by Eq. (25). Eqs(29) and (30) are generally used when a process has been pinpointed, while Eqs(33) and (34) allow one to stand on a largescale window to view the dynamical scenario. The advantage of the latter appears when no *a priori* knowledge of the process is given. We will have opportunities later to see applications of both formalisms.

## 5 Validations

We have validated our theory with a variety of classical benchmark problems. Particularly we have validated with Kuo's barotropic instability model and Eady's model of baroclinic instability, both having (linearized) analytical solutions. In some sense, the application to wake control which we will mention briefly in the next section is also a validation; in fact, that is a more pronounced validation.

The Kuo model (Kuo, 1949; 1973) is about the instability of a 2D jet stream. On an $f$-plane with a coordinate frame with $x$ pointing eastward, $y$ northward, the stream, which is limited within latitudes $y = \pm L$, has a basic profile (Fig. 6a)

$$\bar{u}(y) = \bar{u}_{\max}\cos^2\left(\frac{\pi}{2}\frac{y}{L}\right). \qquad (35)$$

The meridional gradient of its background potential vorticity $q$ is (Fig. 6b)

$$\bar{q}_y = -\bar{u}_{yy} = -\frac{\pi^2}{2L^2}\bar{u}_{\max}\cos\frac{\pi y}{L}, \qquad (36)$$

$\bar{q}_y$ changes sign at $y = \pm L/2$, meeting the necessary condition for instability by Rayleigh's theorem. The formulation and solution of the problem are referred to Kuo's original papers and Liang and Robinson (2007).

We select from the unstable regime a representative mode, and a mode from the neutrally stable regime. Eigenfunctions are accordingly computed and

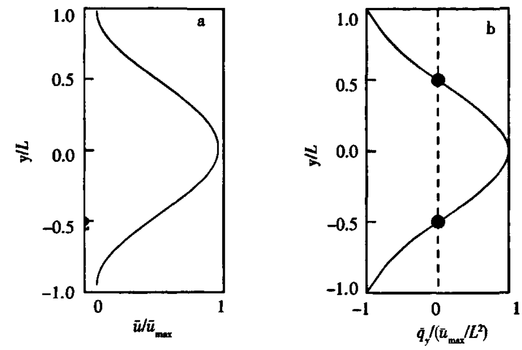


Fig. 6. Configuration of the Kuo model. a. The basic flow profile $\bar{u} = \bar{u}(y)$ and b. the background potential vorticity. Marked are the two inflection points on the profile curve.

the resulting fields are analyzed, using a two-window decomposition with $j_0 = 0$. The large-scale window bound is chosen so as to make contact with the analytical solution. We have found:

(1) when the flow is unstable, $\langle BT \rangle^{\Omega} > 0$;

(2) when the flow is neutrally stable, $\langle BT \rangle^{\Omega} = 0$;

(3) when the flow is stable, $\langle BT \rangle^{\Omega} < 0$.

(Note the averages over the whole domain are necessary since both these benchmark problems are formulated within the classical framework.) These are just one may expect with a barotropic instability. Our formalism is therefore validated with the Kuo model.

The counterpart of the Kuo model is the Eady model (Eady, 1949), which admits only pure baroclinic instability. We thus expect:

(1) when the flow is unstable, $\langle BC \rangle^{\Omega} > 0$, $\langle BT \rangle^{\Omega} = 0$;

(2) when the flow is neutrally stable, $\langle BC \rangle^{\Omega} = \langle BT \rangle^{\Omega} = 0$;

(3) when the flow is stable, $\langle BC \rangle^{\Omega} < 0$, $\langle BT \rangle^{\Omega} = 0$.

In the interest of saving space, it is not our intention to show here how these statements may be verified, but indeed they both turn out to be true

(Liang and Robinson, 2007). Particularly noteworthy is the consistency with the nonlinear result of Liu and Mu (1996) on this problem. The validation with the Eady model is also successful.

## 6 Applications

The theory has been put to application with a variety of real world problems. In this section, we present several examples pertaining to oceanography.

### 6.1 Wake control

The first problem is not from the ocean but has close relation to island wakes (probably has analogy in the East China Sea north of Taiwan, China). We briefly mention it here because it on one hand brings new hope to the field of turbulence control in mechanical and aerospace engineering, on the other hand provides a good validation of our instability theory.

A flow passing a bluff body generates a street of vortices (Karman vortex street) if the Reynolds number lies within a certain range. The vortex shedding exhausts a significant portion of energy and applies an apparent drag on the body. To save energy, a variety of techniques have been proposed to suppress the shedding and hence reduce the drag (Huerre and Monkewite, 1990). But it is still an unexplored area where to place the control for a most efficient suppression. Our theory comes to help at this point. We argued in Liang et al. (2008) and Liang and Wang (2004) that the optimal location for control, in terms of energy saving, is where the absolute instability takes place as the eddies are shedded. This location might vary with time, and it is generally not in accordance to where perturbation energy maximizes. But anyhow our localized hydrodynamic instability analysis allows us to trace it, even in a real time mode, and place the control. The control result turns out to be most efficient: The vortices can be completely suppressed with less energy in comparison to previous experiments such as those in Oertel (1990).

### 6.2 Variability of an open ocean front

The development of MS-EVA was originally motivated by the complex frontal variability observed in the Iceland-Faeroe region, which is of finite amplitude, and intermittent in space and time. The Iceland-Faeore front, or IFF for short, is a sharp temperature and salinity gradient separating the two major world oceans, the Arctic and the North Atlantic (Fig. 7). Its importance has been realized not only from the oceanographic community, but also from industry and military. A historic account can be found in Hopkins (1988), and some recently published papers such as Robinson et al. (1996), Miller and Lermusiaux (1996), and references therein.

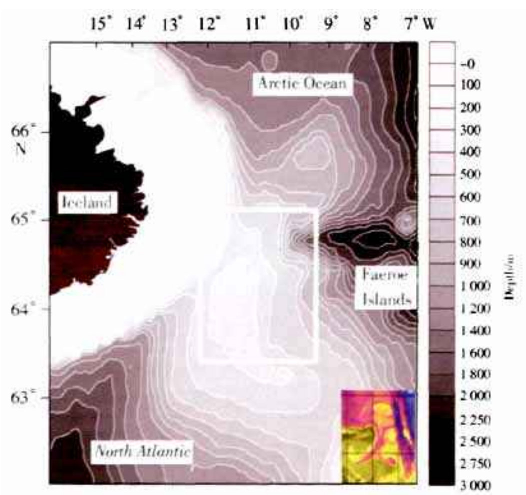


Fig. 7. Bathymetry and geography of the Iceland – Faeroe region. Framed in the middle is the research domain, and overlapped at the lower – right corner is a satellite image of the sea surface temperature observed in this domain on 22 August 1993 [adopted from Liang and Robinson (2004)].

The IFF is observed highly variable. Intrusions in the form of hammerhead or mushroom appear frequently along the frontal axis. In the past three decades, a major theme of the IFF study is to under-stand the dynamical processes underlying these intrusions. Different footprints on a variety of diagnostic fields (usually with complicated pattern) have revealed that the variability might be due to some intrinsic reason, most probably a baroclinic instability (Miller et al., 1995; Millerbrand and Meinck, 1980). But it had not been clear how the dynamical processes work together to drive the intrusions until the MS-EVA study by Liang and Robinson (2004).

Liang and Robinson's study is based on an unprecedented dataset collected by Harvard University in cooperation with the NATO SACLANT Undersea Research Center during the August 1993 Naval RV *Alliance* cruise (Robinson et al., 1996). This set captures a chain of processes toward the formation of a large meandering as shown in the inserted satellite image of Fig. 7. With it Liang and Robinson performed a hindcast to reproduce the frontal evolution (Liang and Robinson, 2004), then had MS-EVA applied to computing the metrics *BC* and *BT*. The application is straightforward, as the theory is real problem-oriented and is platform independent. One first needs to determine the scale windows, with characteristic time series extracted from the dataset, then send the window bounds, together with the model configuration, as inputs to the MS-EVA package (which has been standardized) for results. Refer to Liang and Robinson (2004) for the scale window determination.

The computed metrics show that the IFF variability is mainly reconstructed on the mesoscale window (with scales between 0.7 day and 2.7 days), and appears pronounced in the deep layer. In comparison to *BC*, the barotropic transfer *BT* is negligible. Shown in Fig. 8 is the evolution of *BC* at depth 300 m. An observation is that the computational domain is characterized by a clear-cut (almost) solitary positive BC center. This simple pattern is in distinct contrast to what previous people observed with their diagnostics. Clearly, underlying the complex August 1993 frontal variability is a simple baroclinic instability. Moreover, the transferred potential energy from the large-scale window to the mesoscale window is calculated to be 160 kJ/(m · s) on 17 August to 400 kJ/(m · s) on 21 August at this depth.

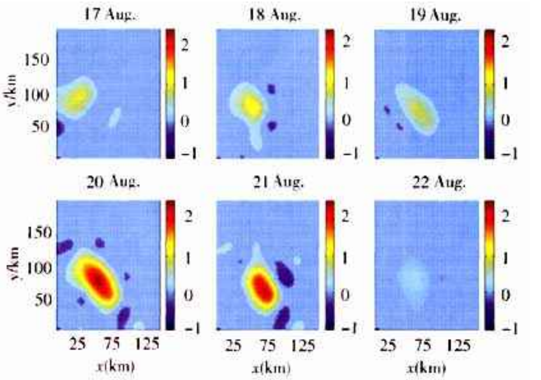


Fig. 8. A time sequence of the 300 m *BC* computed for the Iceland – Faeroe region from 17 August 1993 to 22 August 1993. Positive values indicate baroclinic instability. The units are in $10^{-7}$ $m^2/s^3$. Note 22 August is the day when the large meandering matured. (Recomputed from Liang and Robinson (2004) with the updated more accurate software).

The baroclinic instability has left footprints on the mesoscale field reconstructions. Contoured in Fig. 9 are the mesoscale vertical velocity (upper) and the mesoscale density anomaly (lower) on a meridional section across the hammerhead intrusion. The counter tilting pattern of the former versus the latter is just the evidence of an Eady-like baroclinic instability (see Holton, 1992).

More information about the baroclinic instability can be gleaned by looking at the motion of the *BC* hotspot. It has been justified that the movement of *BC* and/or *BT* corresponds to convective instability, while a stationary positive *BC/BT* center implies absolute instability. Convective instability and absolute instability are the two basic forms of instability which have been studied extensively. In the MS-EVA framework, they are naturally embedded and appear

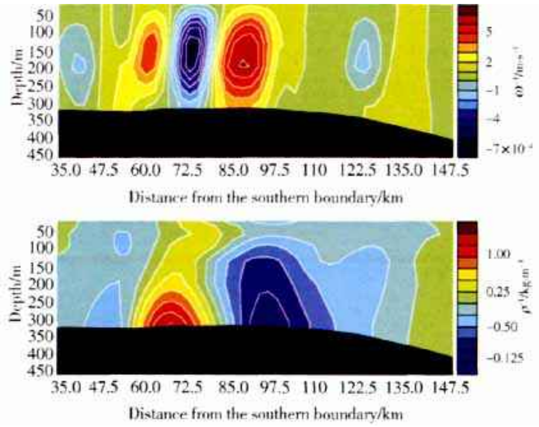

Fig. 9. Distributions of the mesoscale vertical velocity ($\omega^{\sim 1}$) and density anomaly ($\rho^{\sim 1}$) on a meridional section across the hammerhead IFF meandering [ adapted from Liang and Robinson(2004) ]. The counter - tilting trend is an indication of baroclinic instability ( Holton, 1992).

to be simple. In this IFF study, the *BC* hotspot first resides near the western boundary, then moves into the interior and stays there until it disappears. So the baroclinic instability first appears in the form of a convective instability, then switches into a form of absolute instability; accordingly the variability is first in a spatially growing form, which is then switched into a temporally growing pattern. The whole process turns off on 22 August, the day when the hammerhead meandering matures.

The above study is with a specific front. The processes unraveled, however, are generic for ocean front dynamics—In fact, hammerhead meanderings or mushroom intrusions are ubiquitous with ocean fronts. The importance of these processes, including the convective instability, the absolute instability, and the switching between the two, has been testified in a numerical experiment study. We have observed that, for a faithful simulation of the meandering intrusion, a correct reproduction of the convective instability and the absolute instability in appropriate strength with adequate timing is a must.

## 6.3 Dynamics of the Monterey Bay circulation

Another application of the MS-EVA and the MS-EVA-based hydrodynamic instability analysis is for the Monterey Bay circulation. We use the alternative instability formalism [ Eqs(33) and (34) ] to fulfill this study.

Monterey Bay is a crescent-shaped embayment located southwest of San Francisco, California (Fig. 10). Although on a large scale the California coastal current variability is dominated by coastal trapped waves and is relatively clear ( Brink, 1991), on the bay scale the flow is very complex. The curved coastline, the irregular topography, the highly variable forcing, and furthermore, the large submarine valley splitting the domain into two halves, pose a great challenge to the dynamics study ( Rosenfeld et al., 1991). Although efforts have been continuingly invested since 1930 ( Bigelow and Leslie, 1930), the dynamical processes underlying the complex flows are still not clear.

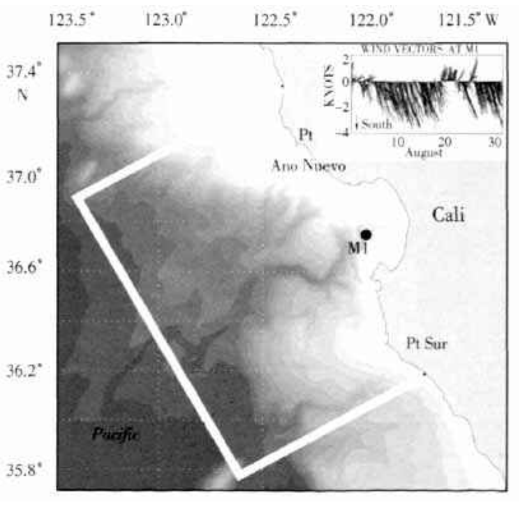


Fig. 10. Research domain for AOSN-II experiment around the Monterey Bay, California. Marked within the Bay is the mooring station M1(36.755°N, 122.025°W). The wind measured at M1 are shown in the inserted stick plot at the northeastern corner. [ Figure adapted from Liang and Robinson(2008) ].

The recent work by Liang and Robinson (2008) makes a breakthrough. They set up an MS-EVA application with a dataset collected from a multiinstitutional multiplatform comprehensive experiment of observation and forecast during August-September 2003, called AOSN-Ⅱ (Autonomous Ocean Sampling Network-Ⅱ) conducted in this region. The research domain is as marked in Fig. 10, which has dimensions 123 km × 144 km. Here we just briefly present part of the results which are relevant to this review; for the MS-EVA setup and other details, the reader is referred to their original paper.

The complexity of the Monterey Bay circulation is found to be due to a mixed instability, with the baroclinic and barotropic transfers of the same order. Look at the *BC* only (*BT* has a similar evolutionary pattern). Figure 11 presents a sequence of the BC spanning the wind relaxation. From it this instability has a bimodal structure, with one center north of the Bay, while another center sitting outside Point Sur near the southwestern corner. For convenience, these two centers will be referred to as, respectively, the Bay mode and the Point Sur mode. Both of them vary as time goes on from 11 August to 23 August, but their evolutions are complementary: One increases with time (Bay mode); another decreases with time (Point Sur mode). If one examines the external forcing variation over this period (Fig. 10), the former is established when the wind relaxes, while the latter is directly driven by the wind. Either way, the wind instills energy into the ocean, which is stored within the largescale window and then released to fuel mesoscale processes. The whole process is summarized in the cartoon in Fig. 12.

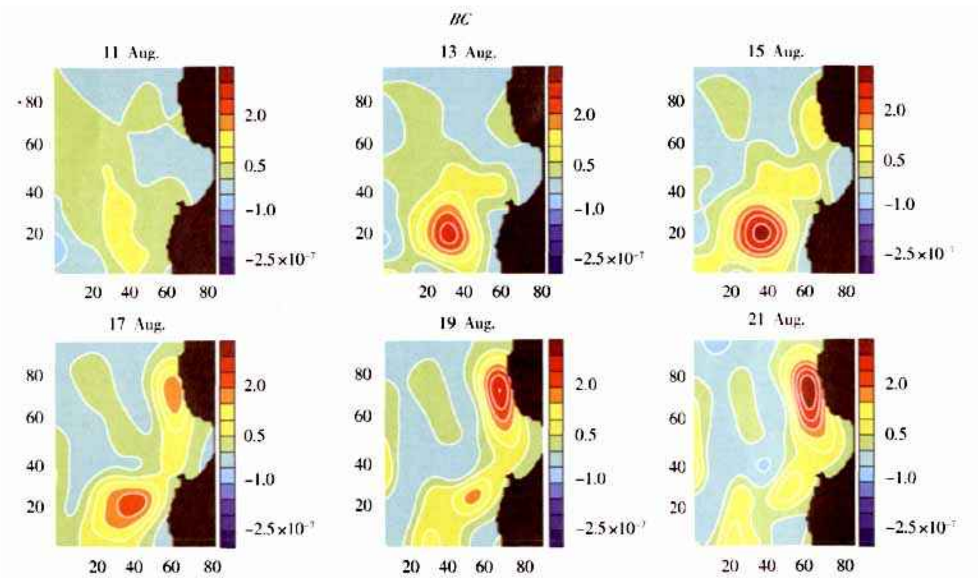


Fig. 11. Surface *BC* (in $m^2/s^3$) evolution during the August 2003 AOSN—II experiment period [adapted from Liang and Robinson (2008)]. The domain has been rotated clockwise by 30°. Coordinates are in grid points ($\Delta x = \Delta y = 2.5$km). The transfer is computed using the alternative formalism [Eqs. (33) – (34)], positive values indicating instability.

As an aside, this work was originally motivated by an abnormally cold water pool often observed over the submarine valley in the Bay. The MS-EVA result shows that the pool in August 2003 is due to a secondary upwelling induced by nonlinear instability. As schematized in Fig. 12, these cold events, once

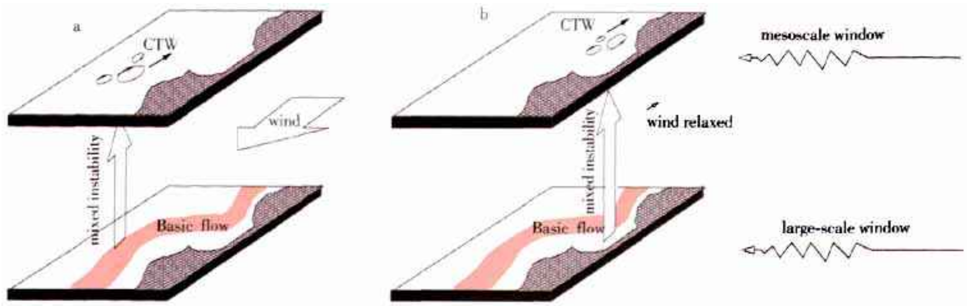


Fig. 12. A cartoon showing the surface processes occurring during August 2003 in the region of Monterey Bay, California. CTW stands for coastal trapped waves. This figure is adapted from Liang and Robinson (2008) with important processes enhanced.

formed, are propagated northward in the form of coastal trapped waves (CTW).

## 7 Discussion and conclusions

A real problem-oriented and self-contained system has been developed for the interpretation of ocean and atmosphere processes from both observation and numerical simulation, which are in nature highly nonlinear, multiscale interactive, and intermittent in space and time. This research involves construction of a mathematical apparatus, multiscale window transform (MWT), and a novel methodology called localized multiscale energy and vorticity analysis (MS-EVA). A theoretical application of the MS-EVA is the formalization of a localized hydrodynamics instability analysis, which makes the study of barotropic instability and baroclinic instability straightforward. The whole theory has been validated with benchmark models, and put to application with real ocean and engineering problems.

The construction of the MWT is to overcome a dilemma between multiscale decomposition and energy localization, and to allow for scale-free processes to be faithfully represented. It is an orthogonal subspace decomposition with respect to scale windows, a generalization of the simple mean-departure separation, but with more scale ranges and nonstationary backgrounds. Properties have been explored and comparisons made with other localized transforms.

The MWT provides a framework for the development of the MS-EVA. The concept of multiscale conversion, multiscale transport, and perfect transfer are naturally introduced, with the aid of a technique called transport-transfer separation. A perfect transfer is a mere redistribution of energy among scale windows, with the total energy conserved. The mathematical rigor and physical robustness make the MS-EVA applicable to problems of arbitrary dynamical setting and geometric configuration.

On the basis of the MS-EVA we have formalized a localized hydrodynamic instability analysis to allow for the application of instability analysis to real problem datasets from observations, numerical simulations, or experiments. The concepts of barotropic instability and baroclinic instability are recast within the MWT framework, and field-like instability metrics obtained. The formalism is generic, Eulerian, and applicable to finite amplitude instabilities with varying backgrounds. It has been validated with several benchmark instability processes.

The power of MS-EVA and the MS-EVA-based instability theory has been demonstrated in a variety of real problem applications. We have successfully used it to get the wake behind a circular cylinder under effective control. The optimal control strategy, which is proposed in terms of the instability metrics, opens a door to a promising field of turbulence control in mechanical and aerospace engineering.

The power of the system has also been demonstrated in two real ocean applications supplied particularly for oceanography research. The first one is about the variability of an open ocean front, the Iceland-Faeroe front (IFF), and particularly the formation of a hammerhead meandering intrusion. We found that the meandering is reconstructed on a meso-scale window. The underlying process can be described as a two-step mechanism. Initially the perturbation is introduced from the western boundary, which amplifies into the interior as a convective instability. Whenever the perturbation grows up to a certain magnitude, the spatial amplification halts, and switches into an instability absolute in character. Accordingly the spatial amplification is locked into a temporally growing mode. The whole process lasts for about 5 days, disappearing just by the day when the meandering intrusion matures. This research has shedded light on the complicated dynamics of frontal meandering, and has since provided a clue to the simulation of highly variable open ocean fronts.

Another ocean application is a dynamical study of the August 2003 circulation around the Monterey Bay, California. It is found that the flow pattern is very complex, and the complexity is due to two instabilities located respectively west of Point Sur and north of the Bay. The two centers forms a bimodal structure, but their underlying driving mechanisms are distinctly different. The former appears when the upwelling favorable wind applies, while the latter is established as the wind relaxes. Both of these instabilities are of finite amplitude, and mixed in type. The resulting mesoscale eddies propagate northward in the form of coastal trapped waves. Secondary upwellings are generated and the cold events are brought northward along the coast.

Potential applications of MS-EVA may be equally sought in other areas. For example, it has been suggested that it could be utilized for the subgrid process parameterization in large eddy simulation (Wang M, private communication), in place of the conventional formalisms in terms of Reynolds stress; it may also be used in other fields of geophysical or environmental fluids, such as the multiscale transport of chemical constituents and pollutant dispersion. We have particularly proposed a prospective application in data assimilation (unpublished manuscript), a growing field which is very important in ocean modeling and parameter estimation. Presently, data assimilation is a scheme of optimization to minimize the state variable mismatch between observation and simulation. However, it is not impossible that the fundamental dynamical processes may be hurt upon taking in data, and accordingly one may cast doubt on the "optimal" posterior field thus obtained. The basic idea of our proposal is to assimilate "processes" rather than "fields", in order that the physics be kept consistent. In an ocean dominated by multiscale dynamical processes, this is made possible with the MS-EVA quantities or metrics. The performance functional is then translated into the mismatch between the processes on both sides, which is expressed in terms of the field-like process metrics we have shown before. We are therefore extending the data assimilation to this functional.

## *Acknowledgements*

This paper was presented at a conference meeting in celebrating Professor Su Jilan's 70th birthday. The author thanks Dr. Huang Daji, Dr. Chen Dake, and many others for their efforts in making the celebration a memorable experience.

# References


Bigelow H B, Leslie M. 1930. Reconnaissance of the waters and plankton of Monterey Bay, July 1928. Bulletin of the Museum of Comparative Zoology at Harvard College, 70: 427 ~ 581

Brink K H. 1991. Coastal-trapped waves and wind - driven currents over the continental shelf. Annu Rev Fluid Mech, 23: 389 ~ 412

Chakrabarti S K. 1989. Standing Rankine - Hugoniot shocks in the hybrid model flows of the black hole accretion and winds. Astrophys J, 347(1), 365 ~ 372

Chorin A J. 1994. Vorticity and Turbulence. Springer. 174

Chu M S, et al. 1996. Resistive interchange modes in negative central shear tokamaks with peaked pressure profiles. Phys Rev Lett, 77(13), 2710 ~ 2713

Cushman-Rosin. 1994. Introduction to Geophysical Fluid Dynamics, Prentice Hall, 320

Drazin P G, Reid W H. 1982. Hydrodynamic Stability. Cambridge University Press, 527

Eady E T. 1949. Long waves and cyclone waves. Tellus, 1: 58 ~ 277

Holschneider M. 1995. Wavelets: An Analysis Tool. Oxford: Clarendon Press, 423

Holton J R. 1992. An Introduction to Dynamic Meteorology. Academic Press. 496

Hopkins T. 1988. The GIN Sea: review of physical oceanography and literature from 1972. Saclant Undersea Research Center Rep No. SR - 124. 190

Huang N E, Shen Z, Long S R. 1999. A new view of nonlinear water waves: the Hilbert spectrum. Annu Rev Fluid Mech, 31: 417 ~ 457

Huerre P, Monkewitz P A. 1990. Local and global instabilities in spatially developing flows. Annu Rev Fluid Mech, 22: 473 ~ 537

Kuo H L. 1949. Dynamic instability of two - dimensional non - divergent flow in a barotropic atmosphere. J Meteorl, 6: 105 ~ 122

Kuo H L. 1973. Dynamics of quasigeostropic flows and instability theory. In: Chia - Shun Yih, ed. Advances in Applied Mechanics, v. 13, Academic Press, 247 ~ 330

Liang XS. 2008. Perfect transfer and mean-eddy interaction in incompressible fluid flows. J Fluid Mech (submitted)

Liang X S, Anderson D G M. 2007. Multiscale window transform. SIAM J. Multiscale Modeling and Simulation vol. 6, 437 - 467.

Liang X S, Robinson A R. 2004. A study of the Iceland - Faeroe frontal variability using the multiscale energy and vorticity analysis. J Phys Oceanogr, 34: 2571 ~ 2591

Liang X S, Robinson A R. 2008. Multiscale processes and nonlinear dynamics for the Monterey Bay region circulation. J Phys Oceanogr, (in press)

Liang X S, Robinson A R. 2005a. Localized multiscale energy and vorticity analysis: I. Fundamentals. Dyn Atmos Oceans, 38: 195 ~ 230

Liang X S, Robinson A R. 2007. Localized multiscale energy and vorticity analysis: II. Finite-amplitnde instability theory and validation. Dyn Atmos Oceans, 44: 51 ~ 76

Liang X S, Wang M. 2004. A Study of Turbulent Wake Dynamics Using a Novel Localized Stability analysis. Proc Summ Prog, Center for Turbulence Research, Stanford University - NASA Ames Research Laboratory, 211 ~ 222

Liang X S. 2002. Multiscale window transform and energy and vorticity analysis. Harvard Reports in Physical/Interdisciplinary Ocean Science, Rep. No. 66. Harvard University, 1 ~ 411

Lima M, Toh S. 1995. Wavelet analysis of the energy transfer caused by convective terms: application to the Burgers shock. Phys Rev (E), 52(6): 6189 ~ 6201

Lin C C. 1966. The Theory of Hydrodynamic Stability. Cambridge University Press, 155

Liu Y M, Mu M. Nonlinear stability theorem for Eady's model quasigeostrophic baroclinic flow. J Atmos Sci, 53, 1459 ~ 1463

Lozano C J, et al. 1996. An interdisciplinary ocean prediction system: Assimilation strategies and structured data models. Reports in Meteorology and Oceanography: Harvard Open Ocean Model Reports. Harvard University

Miller A J, et al. 1995. Quasigeostropic forecasting and physical processes of Iceland - Faeroe Frontal variability. J Phys Oceanogr, 25: 1273 ~ 1295

Miller A J, Lermusiaux P J F. 1996. A topographic Rossby mode resonance over the Iceland-Faeroe Ridge. J Phys Oceanogr, 26: 2735 ~ 2747

Oertel H Jr. 1990. Wakes behind blunt bodies. Annu Rev Fluid Mech, 22: 539 - 558

Pedlosky J. 1979. Geophysical Fluid Dynamics. Springer-Verlag, 624

Pierrehumbert R T, Swanson K L. 1995. Baroclinic instability. Ann Rev Fluid Mech. 27: 419 ~ 467

Pinardi N, Robinson A R. 1986. Quasigeostropic energetics of open ocean regions. Dyn Atmos Oceans, 10: 185 ~ 219

Robinson A R, Miller A J, Warn-Varnas A, et al. 1996. Real-time operational forecasting on shipboard of the Iceland-Faeroe frontal variability. Bull Amer Meteor Soc, 243 ~ 259

Rosenfeld L K, Schwing F B, Garfield N, et al. 1994. Bifurcation flow from an upwelling center: a cold water source for Monterey Bay. Cont Shelf Res, 14: 931 ~ 964

Spall M. 1989. Regional primitive equation modeling and analysis of the POLYMODE data set. Dyn Atmos Oceans, 14: 125 ~ 174

Temam R. 1997. Infinite-Dimensional Dynamical Systems in Mechanics and Physics. New York: Springer, 648

Vanag V K, Zhabotinsky A M, Epstein I R. 2001. Oscillatory clusters in the periodically illuminated, spatially extended Belousov-Zhabotinsky reaction. Phys Rev Lett, 86: 552 ~ 555

Willebrand J, Meinck J. 1980. Statistical analysis of fluctuations in the Iceland-Scotland frontal zone. Deep-Sea Res, 27A: 1047 ~ 1066